Nanomechanical and tribological behavior of hydroxyapatite reinforced ultrahigh molecular weight polyethylene nanocomposites for biomedical applications

Seyed Ali Mirsalehi,[1] Alireza Khavandi,[1] Shamsodin Mirdamadi,[2] M. Reza Naimi-Jamal,[3] Seyed Mohammad Kalantari[1]

[1]Composite Laboratory, School of Materials Science and Engineering, Iran University of Science and Technology, Narmak, Tehran 16846-13114, Iran
[2]Center of excellence for high strength alloys technology (CEHSAT), Department of Metallurgy and Materials Engineering, Iran University of Science and Technology, Narmak, Tehran 16846-13114, Iran
[3]Research Laboratory of Green Organic Synthesis and Polymers, Department of Chemistry, Iran University of Science and Technology, 16846-13114, Tehran, Iran
Correspondence to: M. R. Naimi-Jamal (E-mail: naimi@iust.ac.ir)

ABSTRACT: A hydroxyapatite (HA) particulate reinforced ultrahigh molecular weight polyethylene (UHMWPE) nanocomposite is fabricated by internal mixer at 180°C and using of paraffin oil as a processing aid to overcome the high viscosity of melted UHMWPE. The reinforcing effects of nano-HA are investigated on nanomechanical properties of HA/UHMWPE nanocomposites by nanoindentation and nanoscratching methods. Results show that the nanocomposite with 50 wt % nano-HA exhibits a Young's modulus and hardness of 362.5% and 200% higher, and a friction coefficient of 38.86% lower than that of pure UHMWPE, respectively. © 2015 Wiley Periodicals, Inc. J. Appl. Polym. Sci. **2015**, *132*, 42052.

INTRODUCTION

The nanoindentation method is a powerful and advanced way for measuring hardness and elastic modulus of bulk and nano-featured materials. In addition, the nanoscratching test is a high tech method to measure tribological properties such as coefficient friction of such materials.[1–5] These techniques were introduced in 1992 by Oliver and Pharr[6] and have been widely used to evaluate the mechanical and tribological properties of polymers and composites.[1–5] For example, Shokrieh et al.[1] have reported the nanoindentation and nanoscratch investigations on graphene-based nanocomposites and found that the elastic modulus and normal hardness of graphene-based nanocomposites were improved by adding more graphene nanoplatelets (GNPs) into the polymer matrix.[1] Naimi-Jamal et al.[5] have recently reported that interphase evaluation was possible by investigation of nanomechanical responses of UHMWPE/SCF/nano-SiO$_2$ hybrid composites in different phases. They found that the nanomechanical properties of the polymeric matrix and interphase regions showed significant differences in reduced Young's modulus and hardness.[5] However, little investigations

have been carried out for studying the nanomechanical and tribological properties of nanocomposites.

In conventional nanoindentation method, a small tip is pressed into a sample with a known load (force) and retracted sequentially, which generates a force–displacement curve.[6,7] The nanoscratching test is also performed using a two-dimensional nanoindentation machine at a chosen normal load (F_N), while shearing by the required lateral force (F_L) for the scratching and with a known constant scratching speed and length.[8,9]

Many composite materials, including ceramic matrix and polymer matrix composites have been developed for biomedical applications. Current polymer processing technology makes it possible to produce highly filled polymers of excellent quality, which enables us to manufacture bioactive, high performance ceramic/polymer composites as biomaterials.[10–13] Among the others, the polymer–matrix composites are widely used in engineering, due to their much smaller weight, good mechanical properties, better corrosion resistance and biocompatibility than the metal–matrix and ceramic–matrix composites. For example,

ultra-high-molecular weight polyethylene (UHMWPE) has been widely used in bearing applications due to its good chemical stability, biocompatibility, friction-reducing and antiwear ability.[14] UHMWPE is a kind of high density polyethylene with an average molecular weight (Mw) of up to several millions g/mol.[15] The short-term advantages offered by UHMWPE include high strength characteristics, very good sliding properties, good fatigue resistance, excellent biocompatibility, low friction factor, high wear resistance, and high chemical resistance in corrosive media. In the long-term implantation, the behavior of UHMWPE is compromised by its insufficient wear performance, low stiffness and high creep compliance. As chemical nature and physical–mechanical properties of UHMWPE are similar to bio-tissues, it is widely used as a material for the manufacturing of implants.[16–20]

Calcium phosphates are primarily used as bone substitutes in biomedical industry due to their biocompatibility, low density, chemical stability, and their compositional similarity to the mineral phase of bone. Hydroxyapatite (HA), having a chemical composition of $Ca_{10}(PO_4)_6(OH)_2$, is a kind of calcium phosphate bioceramic materials. It is one of the most widely investigated bioceramic materials used for bone and tooth substitution applications.[21] Micron-size HA reinforced polymer based implants may be undesirability affected by the interaction with articular fluid resulting to micronsize pore skeleton formation and subsequent lack of wear resistance and strength. In contrast, adding of nanosize HA particles into polymer matrix will prepare porous nanoskeleton, which does not adversely affect mechanical properties and will be accompanied by the reposition of synovial liquid in the pores. This liquid will improve wear resistance of polymer by allocation at the interface of metal head and plastic cup of hip prostheses.[16–18] HA nanoparticles suffer from a high tendency to aggregate. It is generally difficult to manufacture a nanocomposite with nonaggregated nanoparticles, due to the high surface free energy of them. Different mechanical and chemical dispersion techniques have been developed, which can be used to disperse inorganic nanoparticles in organic solvents or resins.[22] Our study describes the use of internal mixer and paraffin oil as a processing aid to disperse nano-HA into UHMWPE.

Many researchers have tried to develop HA reinforced high density polyethylene (HDPE) as bone-analog composites for biomedical applications. As a pioneer, Bonfield et al. have reported the effect of HA on mechanical properties of HA/HDPE composite for bone replacement. They demonstrated that HA effectively reinforced HDPE, with a considerable increase in Young's modulus.[13,23] Although, HDPE has been widely used as matrix for bone-analog composites,[23–25] its mechanical and tribological properties are inferior to UHMWPE. The low mechanical properties of HA/HDPE composites have limited their applications as bioimplants. Therefore, the use of UHMWPE as a composite matrix has been developed for such applications. Many researchers have reported on mechanical and biological properties of UHMWPE as matrix in biocomposites. For example, the HA/UHMWPE composites for orthopedic applications were evaluated by Liming et al.[26] They presented a novel processing method of combining ball milling and swelling for fabricating

HA/UHMWPE biocomposite. Knets et al. investigated on natural HA/UHMWPE composite for replacement of bone tissue. They found that elastic modulus was enhanced by a higher percentage of natural HA, but deformation was decreased.[27] Filipenkov et al.[28] determined the mechanical characteristics and biocompatibility of natural hydroxyapatites (NHA)/UHMWPE composites as bone replacement. They stated that a change in the matrix to reinforcement ratio would change the mechanical properties of NHA/UHMWPE composites.

In this study, we tried to manufacture HA/UHMWPE nanocomposites and investigate on their nanomechanical and tribological properties as a candidate for bone substitute. At First, HA/UHMWPE nanocomposites were fabricated by internal mixer and then nanomechanical and tribological characteristics of HA/UHMWPE nanocomposites were measured by nanoindentation and nanoscratch methods. Results show that the composite with 50 wt % nano-HA exhibits a Young's modulus and hardness of 362.5% and 200% higher, and a friction coefficient 38.86% lower than that of pure UHMWPE, respectively.

EXPERIMENTAL

Raw Materials
Nano-HA powders were synthesized by sol-gel method from analytical grade calcium nitrate tetrahydrate $Ca(NO_3)_2.4H_2O$ [Merck] and phosphoric pentoxide P_2O_5 [Merck]. The matrix was UHMWPE with a weight average molecular weight of 6×10^6 g/mol (0.94 g/cm^3 at 25°C, Sigma-Aldrich with 429015 trade code). Pharmaceutical grade paraffin oil was used as a processing aid (107174 trade code, 0.86 g/cm^3 at 20°C, Merck, Germany).

Preparation and Characterization of Composites
UHMWPE is usually prepared by a Ziegler–Natta polymerization method at a temperature around 60°C, where chain crystallization rate is much lower than chain propagation rate. The resulting polymer has very large numbers of entanglements. Due to the nature of this process, one mg of this polymer with a million g/mol molecular weight contains ca. 10^{14} entangled chains.[29] Because of this fact, the mobility of the UHMWPE chains is very much limited, resulting in an extremely high melt viscosity of the polymer. To overcome this problem, at first, the sufficient amounts of UHMWPE, required for a given weight fraction in the final composite, was hand-mixed with the liquid paraffin oil at 100°C. The UHMWPE grains absorbed the paraffin oil and swelled. Paraffin oil was used, as it is an inert and nontoxic hydrocarbon lubricant. During the swelling process, the short-chain oligomers of paraffin oil increased the distance between the polymer molecules and led to higher chain mobility. Thus, the viscosity of the system was lowered significantly to a range that allowed mix processing.

The compounding of nano-HA and swelled UHMWPE granules was carried out using a laboratory scale melting mixer (Brabender plastic-corder). All the materials were dried in a vacuum oven for 5 h at 110°C before the melt-mixing process. Then, UHMWPE was fed into the mixing chamber with a rotation speed of 120 rpm at 180°C. After melting, rotation speed of roller was decreased to 80 rpm and nano-HA particles were

Table I. Formulations and Densities of the Composites

Composite	UHMWPE (wt %)	HA (wt %)	Composite density (g/cm^3)
Control	100	0	0.94
A1	90	10	1.166
A2	80	20	1.392
A3	70	30	1.618
A4	60	40	1.844
A5	50	50	2.07

added. The total mixing time was 15 min. Finally, the samples were cooled to room temperature. The same condition was applied to fabricate a pure UHMWPE sample as the control sample.

Extracting Paraffin Oil

For nanomechanical tests, it was necessary to remove the paraffin oil. The removal of paraffin oil was undertaken by a two-step process. In the first step, the obtained materials from compounding were squeezed by hot press at 100°C at a pressure of 3.8 MPa for an hour. Subsequently, the still remaining oil was removed by three times extraction in a soxhlet extractor using acetone. Prior to each extraction step, the sample was cryomilled to enhance the diffusion process of the solvent (acetone). Then, acetone was vacuum evaporated in an oven for 24 h at 100°C. The solid was then grinded by a laboratory scale grinder (Retsch ZM200) into fine powders to improve distribution and dispersion of filler into the matrix. The sample was then compression-molded by a Toyo-seiki machine (Japan) at 200°C under a pressure of 3.8 MPa into cylinders with a diameter of 10 mm and a height of 3 mm for nanoindentation and nanoscratching tests. After 30 min, the cylinders were cooled naturally under the same pressure. Table I summarizes the samples formulations.

Nanomechanical Test Method

Nanoindentation tests were conducted by using a TriboScope® system (Hysitron, USA) nanomechanical test Instrument with a 2D transducer, equipped with a Berkovich type indenter tip according to the procedure described in ISO14577. Samples were polished successively by 0.05 μm diamond suspension to reach a relatively flat surface. A loading-unloading function with a maximum load of 200 μN was used. The load was reached its maximum in 30 s and was removed again in 30 s after a 10 s holding time at peak load (Figure 1). Three samples were manufactured for each composition. To obtain statistically significant results, five indentations were made for each sample at random locations (totally, 15 indentations were carried out for each composition). The reduced elastic modulus and the hardness were calculated from the unloading curve, after calibrating contact area function of the indenter by a quartz standard sample.[30] The hardness (H) is defined as the maximum indentation load (F_{max}) divided by the projected contact area (A_c) of the indentation:[6,30]

$$H = \frac{F_{max}}{A_c} \tag{1}$$

Where, A_c is a function of contact depth (h), which is measured in situ during the test according to the area function calibra-

tion. The stiffness (S) and the reduced elasticity modulus (E_r) are related by the following equations given by Oliver and Pharr:[6,30]

$$E_r = \frac{(\pi)^{\frac{1}{2}}}{\beta} \times \frac{S}{(A_c)^{\frac{1}{2}}} \tag{2}$$

β is a constant, which also depends on the indenter geometry (1.034 for the Berkovich one).[31]

The reduced modulus, E_r is related to the elastic modulus E by:[32]

$$\frac{1}{E_r} = \frac{1-v^2}{E} + \frac{1-v_i^2}{E_i} \tag{3}$$

Where v, E, v_i (0.07), and E_i (1140 GPa) are Poisson's ratio and elastic modulus of the material and indenter, respectively.[32]

The plasticity index (ψ) is a parameter, which is used to evaluate the elastic-plastic behavior of materials under external stress and strain condition. In the nanoindentation test, the plasticity index is related to the area under the loading curve (S_1) (or the total indentation work) and unloading curve (S_2) (or elastic deformation work) by the following equation (Figure 2):[33,34]

$$\psi = \frac{S_1 - S_2}{S_1} \tag{4}$$

Nanoscratching Test Method

Nanoscratching test is used as a representation of tribological behavior of a material's surface. A loading–unloading function with a maximum load of 150 μN was applied (Figure 3). The load was reached its maximum in 5 s, and removed within 5 s after scratching. The scratching time was 30 s. To obtain statistically significant results, three scratches were made for each sample at random locations (totally, nine scratches were performed for each composition). The scratch path was 4.0 μm and the rate of scratching was 0.133 μm/s for all specimens. The normal displacement (depth) and lateral displacement of the indenter tip were recorded, as well as the normal and the lateral force exerted. The parameter μ (friction coefficient) was determined
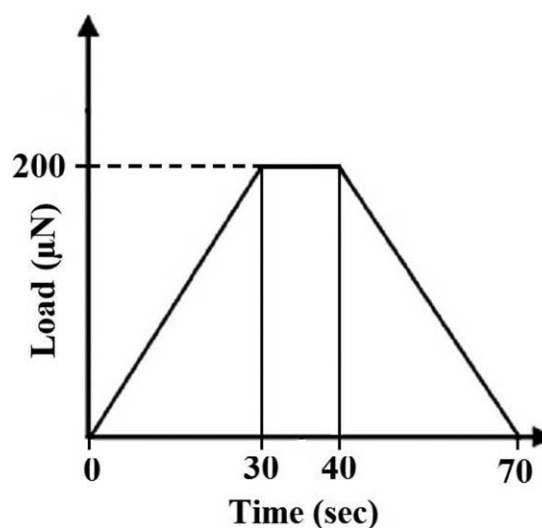

Figure 1. The loading–unloading function with 200 μN as peak load and 30 s for both loading and unloading time with 10 s holding time.
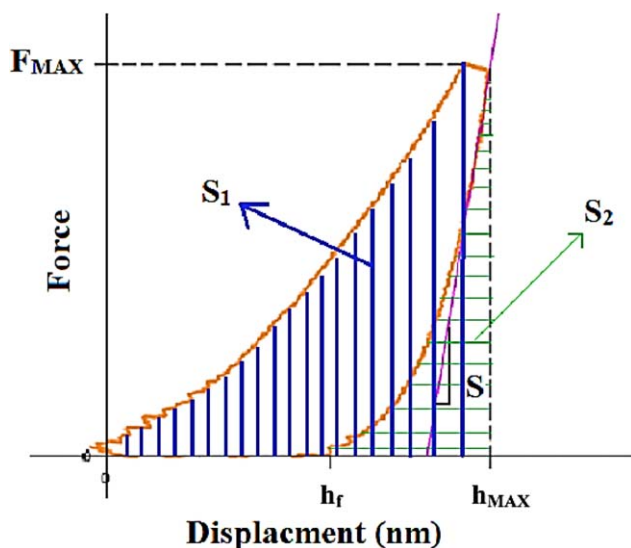
Figure 2. A schematic load–penetration depth curve achieved from a real nanoindentation test (S= stiffness (dF/dh); S_1= the area under the loading curve (total work of indentation); S_2= the area under the unloading curve (elastic work of indentation)). [Color figure can be viewed in the online issue, which is available at wileyonlinelibrary.com.]

by the ratio of lateral force (F_L) over normal force (F_N) data as follows:[5]

$$\mu = \frac{F_L}{F_N} \qquad (5)$$

At the beginning of each scratch, the lateral force changes rapidly from zero. So, to have more consistency in friction coefficients data, the first third part of each scratch was not considered.

RESULTS AND DISCUSSION

Microstructure Characterization

Figure 4 shows the scanning electron microscopy (SEM) evaluations of dispersion states of the nanoparticles into matrix on cross-sections after sputtering a gold layer (with a thickness of 50 nm approximately). As heavy atoms with a high atomic number are stronger scatters than light ones, to highlight HA nanoparticles from the cross-sections of the composite system, a secondary electron (SE) detector was used. Figure 4 demonstrates that nano-HA particles were homogenously distributed by melt-mixing process, but also agglomerated. It occurs because by using nano-HA, the free surface energy and consequently the tendency to interaction between filler nanoparticles increases and this leads to agglomeration of nanoparticles.

Nanomechanical Properties

As it is known, the matrix materials (polymers, metals, and ceramics), the dimensions/shapes of reinforcement (short fibers, particles, and continuous fibers), the reinforcement/matrix ratio, the dispersion states of the filler into matrix, and the adhesion at the filler–matrix interface are the main factors, which affect the mechanical properties of engineering composite materials.[35,36]

The stiffness of composite materials can be improved by adding smaller particle size of filler into the matrix of composite. Fur-

thermore, the stiffness and wear properties of HA/UHMWPE nanocomposites depend on the HA weight fraction. The higher HA content results in higher interactions between the polymer and the filler, which leads to improve strength at breaking, when the implant is under mechanical loading.[11,20,37,38] The influence of adding HA nanoparticles on the hardness, elasticity and scratch resistance of UHMWPE will be discussed in the following.

Nanoindentation Results

Elastic modulus and hardness were calculated from the recorded load–displacement curves in the unloading segment [Figure 5(a)]. The reported value for each composition is the average of 15 different indentations carried out. Figure 5(b and c) show the modulus and hardness of the HA/UHMWPE nanocomposites. Nanoindentation tests were performed at maximum peak normal force of 200 μN, as described before. By increasing nano-HA particles content, load-displacement curves were shifted to the left and the maximum depths were reduced due to the increasing hardness. According to Figure 5(b and c), the incorporation of nano-HA into the polymer matrix significantly increased the elastic modulus and hardness; this is obviously due to much greater elastic modulus and hardness of HA in comparison with UHMWPE. In Figure 5(b), the increasing trend of modulus can be seen as a function of nano-HA content. This fact can be deduced from the loading-unloading curves, because by increasing nano-HA content, the slope of unloading curve has increased. Modulus and the slope of the unloading curve have a direct relationship [eq. (2)] and an increase in stiffness will result in a higher modulus. By adding nano-HA particles into pure UHMWPE, modulus and hardness of the composites were increased due to the incorporating filler with high strength and high aspect ratio.

By adding 50 wt % nano-HA into pure UHMWPE, the modulus increased by 362.5% (3.7 GPa), in comparison with pure UHMWPE (0.8 GPa). The elastic modulus range of spongy and
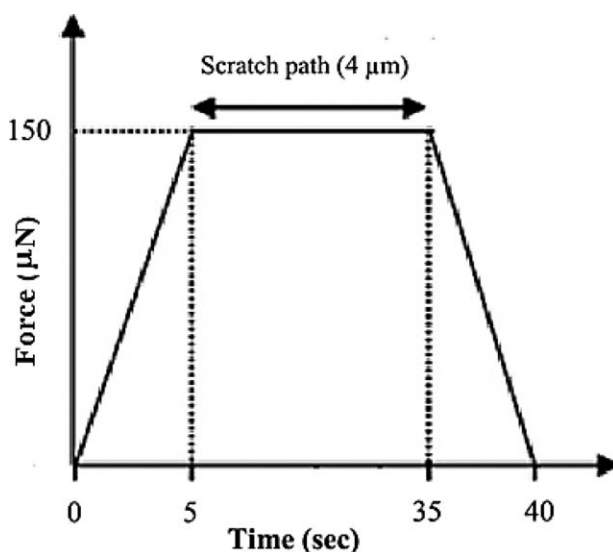

Figure 3. The loading–unloading function with 150 μN as maximum force and 5 s for both loading and unloading time with holding time of 30 s and rate of scratch of 0.13 μm/s.
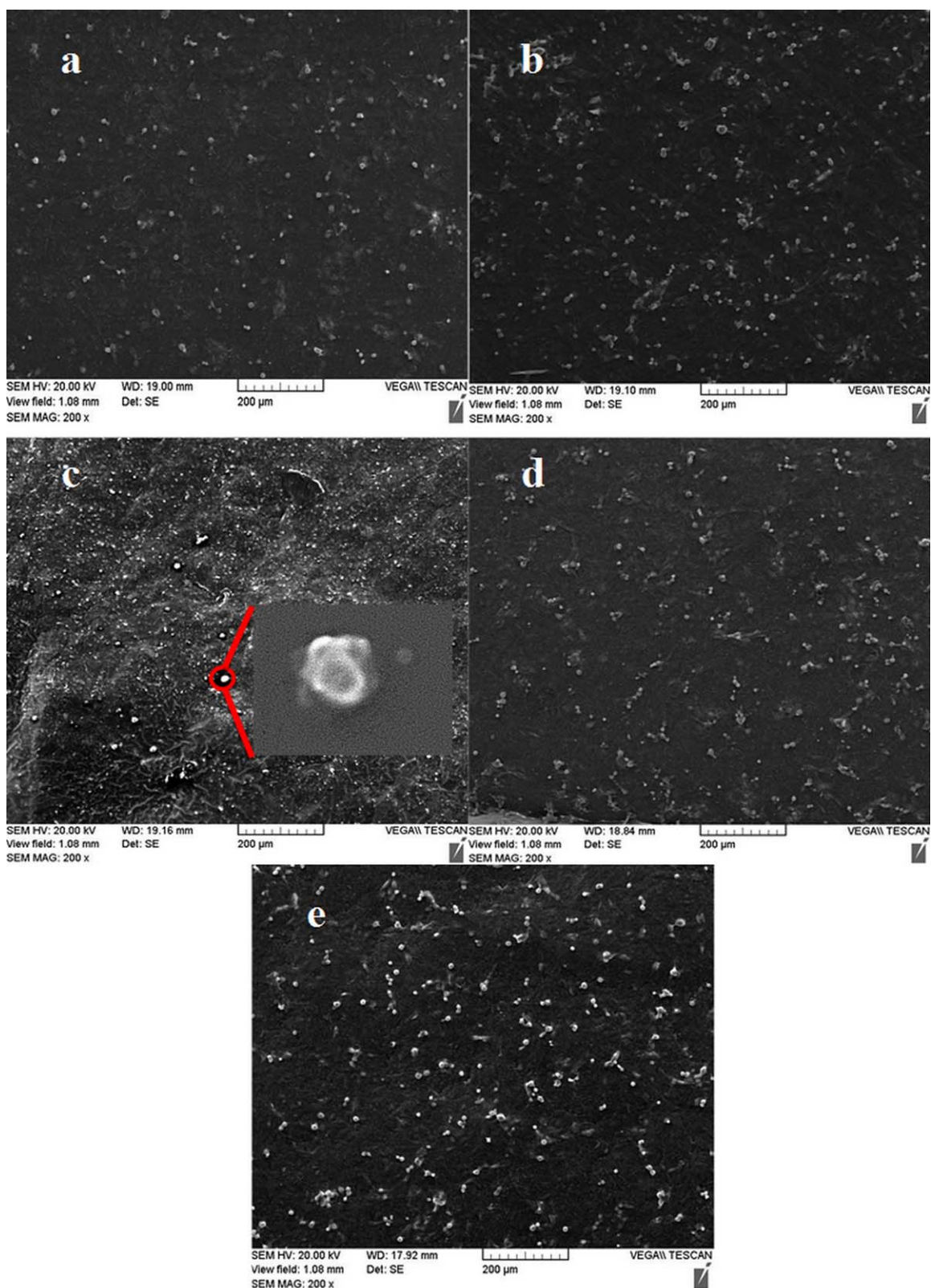
Figure 4. SEM images of cross-sections of (a) A1, (b) A2, (c) A3, (d) A4, and (e) A5 composites. [Color figure can be viewed in the online issue, which is available at wileyonlinelibrary.com.]
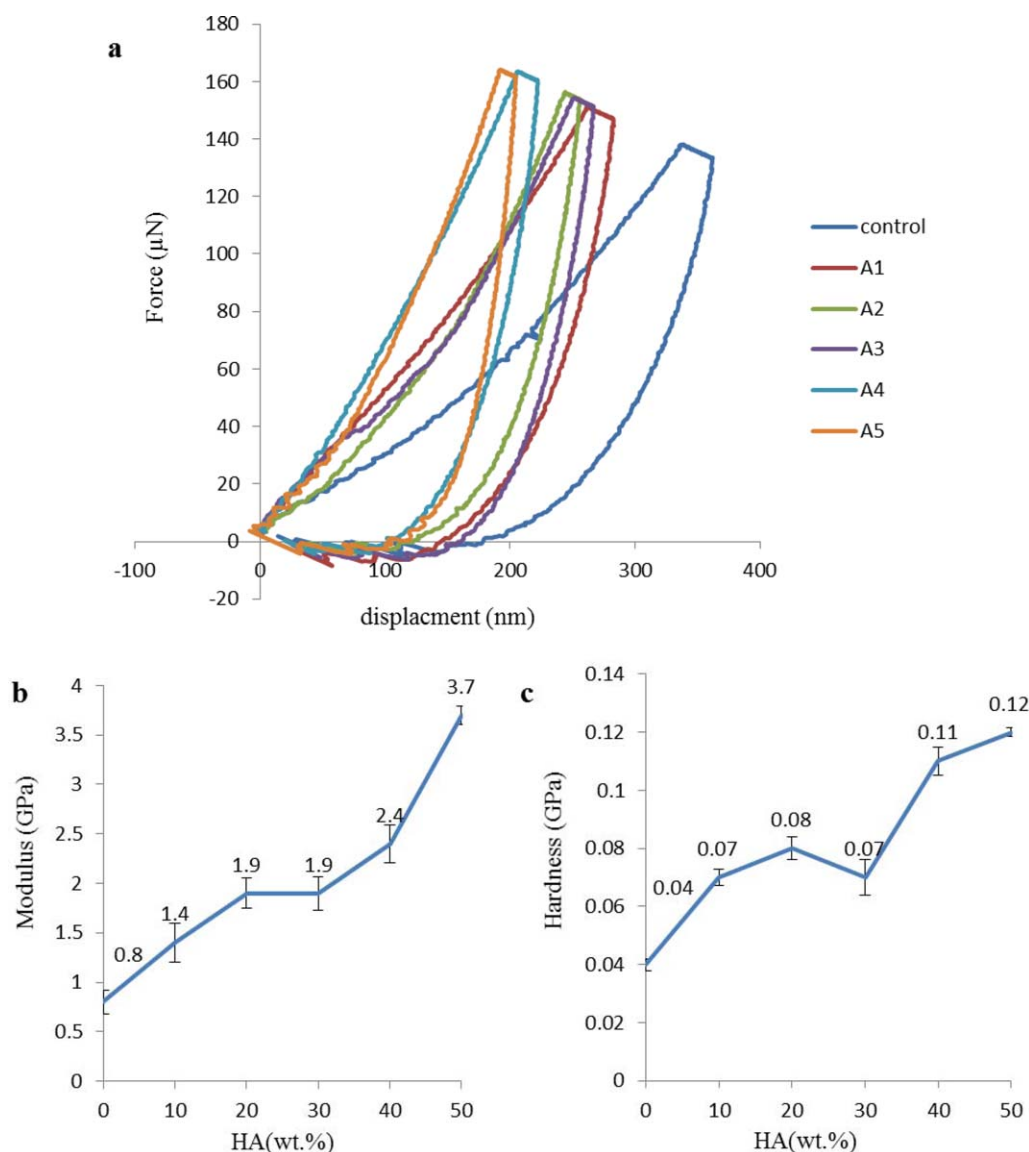
Figure 5. (a) Recorded load-displacement curves, (b) elastic modulus, and (c) hardness data evaluated by 15 indented points for each composition. [Color figure can be viewed in the online issue, which is available at wileyonlinelibrary.com.]

cortical human bone is 0.01–1.57 GPa and 7–30 GPa, respectively.[39–44] Therefore, the elastic modulus of A5 sample is more than spongy bone and less than cortical bone. This sample is then not a good candidate for spongy bone replacement, due to the mismatch of elastic modulus between A5 sample and spongy bones, which will lead to the stress shielding effect. The A1 sample has an elastic modulus (1.4 GPa) close to spongy bone. In elastic modulus term, the A1 sample is more appropriate for spongy bone replacement.

The hardness was also increased by adding nano-HA into the polymer matrix as illustrated in Figure 5(c). By adding 50 wt % nano-HA into pure UHMWPE, the hardness was increased to 0.12 GPa, showing a 200% improvement in comparison with pure UHMWPE (0.04 GPa). As the hardness of a material is defined as the degree of its resistance to plastic deformation,[45,46] the greater hardness of A5 sample compared to control sample

contributes to more resistance of A5 sample to plastic deformation.

As can be seen in Figure 5(b and c), the elastic modulus of A3 sample was the same as A2 sample, whereas the hardness of A3 sample was lower than A2 sample. This fact may be due to poor dispersion of nano-HA in the matrix or experimental error. According to Figure 4, the number of agglomerated nano-HA in A3 sample is more than other samples. On increasing of such aggregated particles, the stress concentration sites increase and the interface area between filler and matrix decreases. Therefore, the efficiency of interfacial bonds for stress transfer was reduced and mechanical properties of A3 sample were decreased.

The results reported in literature are comparable with our study. Liming[26] have reported an average HA (20 vol % or ∼ 50 wt
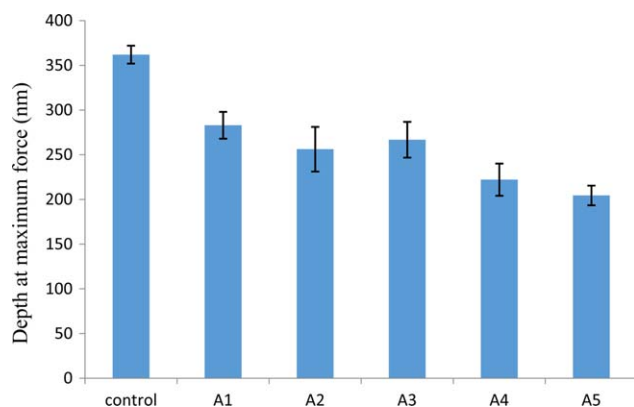
Figure 6. Depths at maximum force during nanoindentations for different compositions. [Color figure can be viewed in the online issue, which is available at wileyonlinelibrary.com.]

Figure 7. Calculated plasticity indexes of nanocomposites. [Color figure can be viewed in the online issue, which is available at wileyonlinelibrary.com.]

%)/UHMWPE composite elastic modulus of 1633 ± 73 MPa. In his study, the modulus showed about 84% enhancement ($E_{UHMWPE} = 887 \pm 41$ MPa). His study was performed by micron-sized HA as the reinforcement.[26] In our study, by adding 50 wt % nano-HA into pure UHMWPE, the modulus revealed about 360% improvement in comparison with pure UHMWPE. This difference in elastic modulus improvement in the same weight percentage of reinforcements is due to the size of the filler. By decreasing the particle size of the filler at a fixed particle weight percentage, more individual particles are present, and the surface area and surface energy are increased and then more efficient interfacial bonds are provided.[26]

Figure 6 shows penetration depths at maximum force for different compositions. According to this figure, the maximum depth was decreased by adding nano-HA into pure UHMWPE. At a peak force of 200 μN, the depth of the indent of control, A1, A2, A3, A4, and A5 compositions were 362, 283, 256, 267, 222, and 204 nm, respectively. This fact indicates that the nanocomposites have more hardness due to an increase of the amount of nano-HA powders into UHMWPE. As can be seen in Figure 6, the value of depth at maximum force of A3 sample is between A2 and A1 samples, which has no special meaning and may be related to poor dispersion of reinforcement into UHMWPE or experimental error, as previously stated.

Plasticity Index

The plasticity index determines the elastic recovery ability of the material after removal of the deformative load. Irreversible work during the nanoindentation test (the plastic work) is determined by the difference between S_1 and S_2. The value of plasticity index (ψ) is between 0 and 1 for viscoelastic-plastic materials such as polymers, while fully plastic and the fully elastic materials have $\psi = 1$ and 0, respectively. Surface roughness and hardness of the material are main factors, which plasticity index depends on them. Usually, soft and rough materials have higher ψ in comparison to other materials.[47] Generally, materials with higher ψ have higher friction wear volume and higher friction coefficient.[48] Figure 7 shows the influence of nano-HA particles on the plasticity index of the specimens. According to Figure 7, the plasticity index of the pure UHMWPE polymer
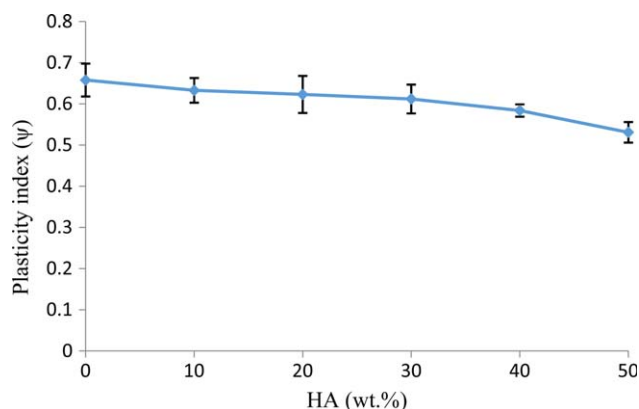
and the nanocomposites was observed to be 0.658, 0.633, 0.623, 0.612, 0.584, and 0.531, respectively. As shown in Figure 7, A5 composite exhibited 19.3% reduction in plasticity index in comparison with pure UHMWPE. The reduction in plasticity index after adding the filler is because the reinforcement improved the hardness and the stiffness of the nanocomposites. It is known that the harder materials have lower plasticity index than the softer materials.[27] The increase in nano-HA content leads to an increase in the interfacial bonding between filler and matrix, and as a result, the stress transfer from polymer to matrix is improved, and thus plasticity index decreases.

Tribological Properties

Nanoscratching Results. The thermoplastic polymers exhibit elastic, plastic, viscoelastic, viscoplastic, and brittle properties, which influence their mechanical properties. Numerous studies on macroscratching and microscratching have been performed in terms of wear and scratch resistance.[9] A nanoscratching test can exhibits a qualitative evaluation of the tribological properties of the material surface. This method was mainly described in detail by Hodzic et al.[49] The F_N and F_L of the indenter tip and also the normal and the lateral displacements were simultaneously recorded. The friction coefficient (μ) is defined as the ratio of the F_L to the F_N. Table II summarizes lateral force (F_L), and normal force (F_N) of the indenter tip and μ of the specimens [eq. (5)]. According to this table, by increasing the amount of nano-HA, the normal displacement and F_L (which can be described as the opposite force applied to the indenter

Table II. Lateral and Normal Forces of the Scratches and Calculated Friction Coefficients of Nanocomposites

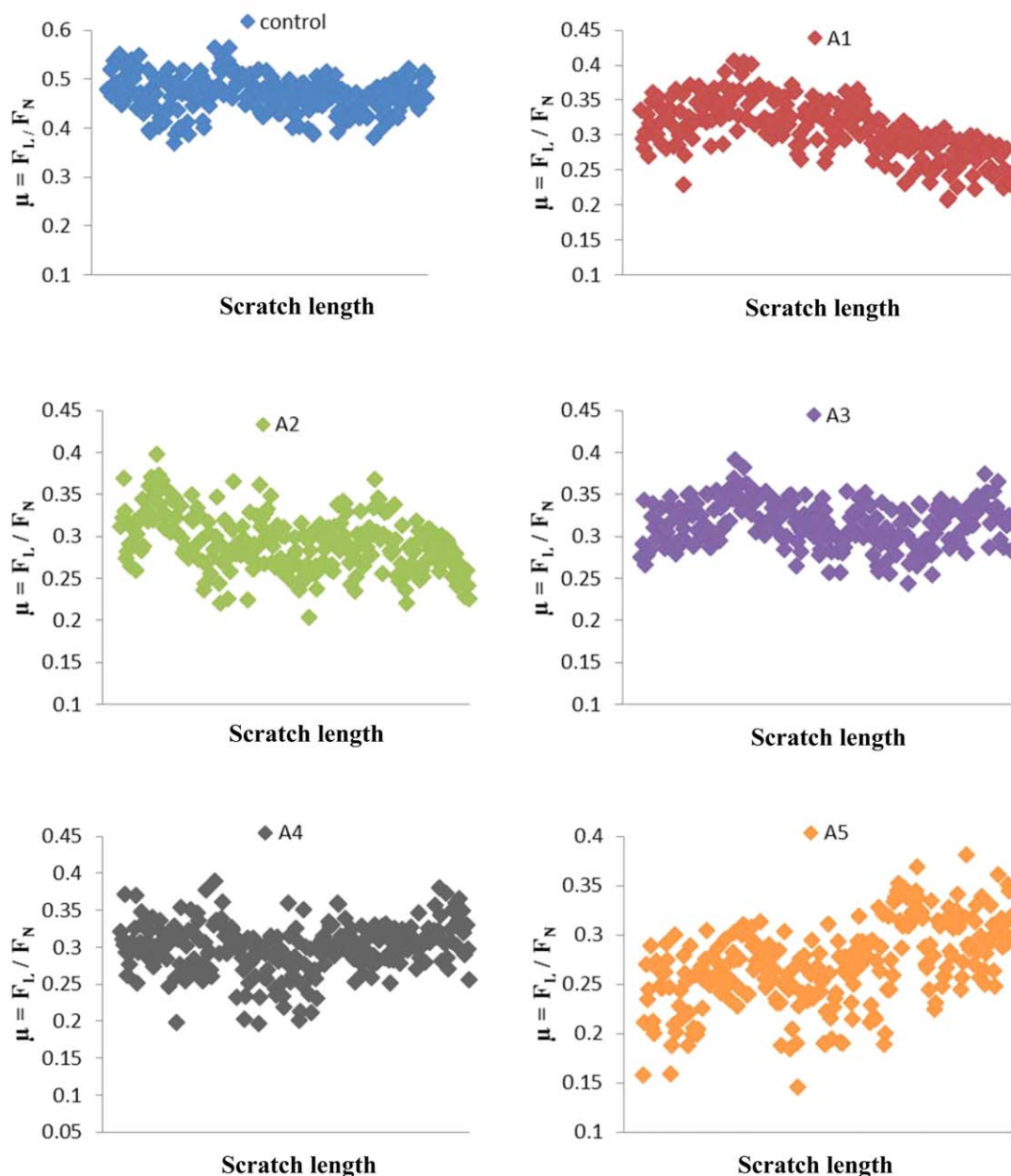| Composite	F_L (μN)	F_N (μN)	$\mu = F_L/F_N$
Control	44.053	92.366	0.476
A1	40.187	121.997	0.329
A2	37.592	114.852	0.327
A3	33.484	111.986	0.299
A4	33.229	113.409	0.293
A5	29.496	101.360	0.291

Figure 8. Friction coefficient (F_L/F_N) variations of composites. [Color figure can be viewed in the online issue, which is available at wileyonlinelibrary.com.]

tip by the sample during the scratching) were decreased, while F_N is principally constant (with some minor fluctuations around 115). This leads to a decrease in μ.

Figure 8 exhibits the friction coefficient of the composites calculated from the nanoscratching tests data. As can be seen in Figure 8, significant deviations in friction coefficient occurred, when control sample was tested. By adding 50 wt % nano-HA into pure UHMWPE, the friction coefficient was measured as 0.291, showing a 38.86% reduction in comparison with pure UHMWPE. This remarkable change indicates significant change in the properties of the scratched material along the scratch path. This phenomenon denotes the effect of nano-HA on the scratch resistance of nanocomposites. In fact, when the tip con-

fronts nano-HA in the scratch direction, it needs more force to move forward. As a result, the tip has to move upward.[1] The nano-HA increases the scratch resistance of nanocomposites not only by individually impeding the tip, but also by improving mechanical properties globally. As discussed, incorporation of nano-HA into the pure UHMWPE improved the elasticity modulus and normal hardness. Therefore, the improvement of these parameters gives better elastic recovery and less deformation under a specified load, hence the coefficient of friction will improve in the nanocomposites.

Adam et al.[50] reported that the maximum friction coefficient between indenter of nanoindentation machine and bone was 0.3 for bone with elastic modulus E=13.56 GPa. Shockey et al.
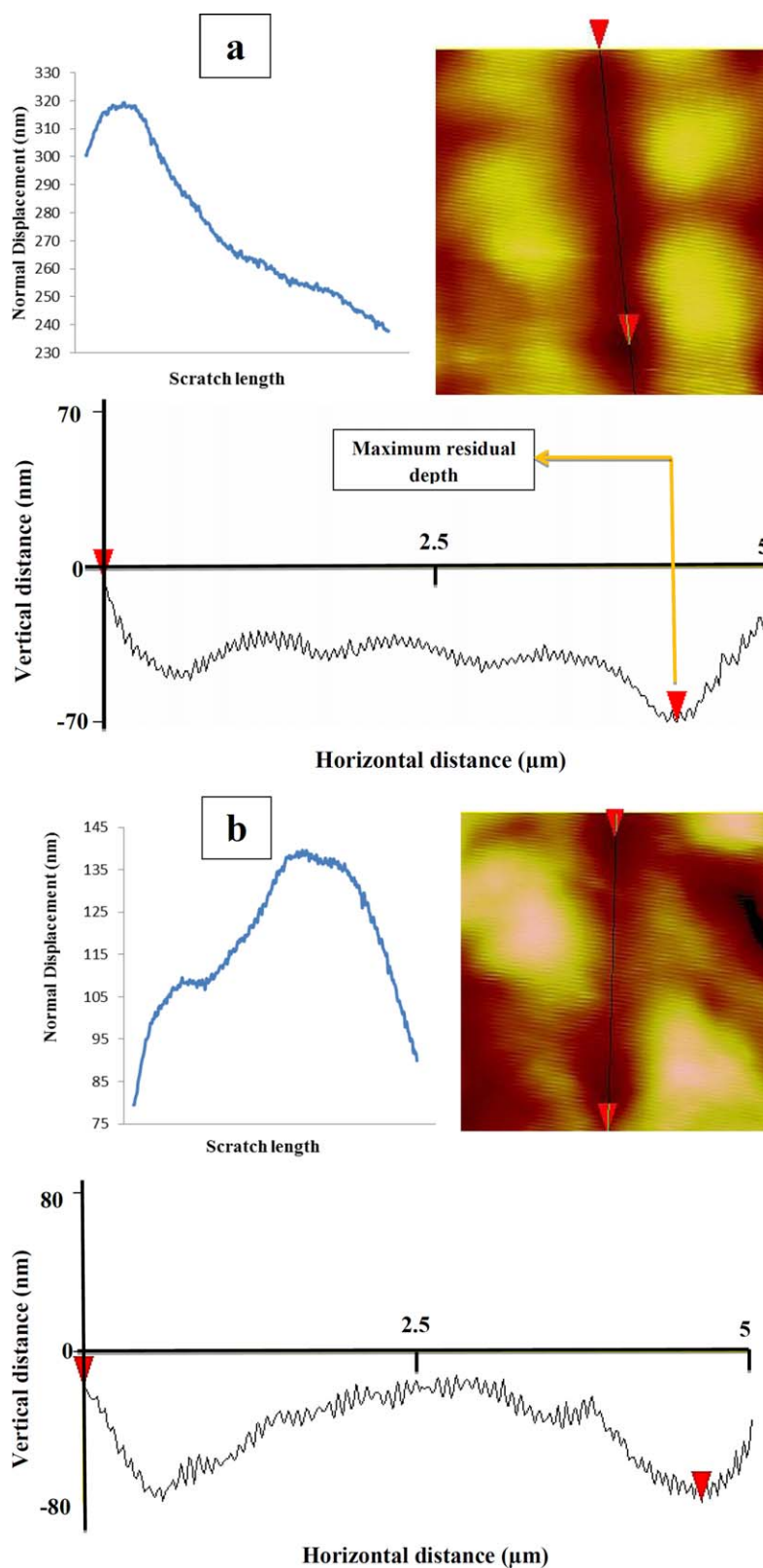
Figure 9. Online penetration depths during the scratching and residual depths of (a) A1 and (b) A5 sample measured from AFM data. [Color figure can be viewed in the online issue, which is available at wileyonlinelibrary.com.]

reported that the friction coefficients range of tibia and femora is 0.372–0.706 and 0.394–0.407, respectively.[51] The friction coefficients of A4 and A5 samples are less than friction coefficients of tibia and femora. Therefore, the A4 and A5 composites are good candidates for bone substitute application, where it is needed to wear-bearing materials with μ less than 0.3.

Figure 9 compares the penetration and the maximum residual depths of A1 and A5 composites. As shown, normal displacement (nm) data versus time (seconds) exhibits in situ penetration depths. In addition, in Figure 9, the vertical distance measured from atomic force microscopy (AFM) data immediately after the scratching test, is the vertical distance between two indicated points in the diagram, which in turn illustrates the maximum residual depth of the scratch. According to this figure, the maximum penetration and maximum residual depth of the A1 and A5 samples were observed to be 319.4, 65.834 (online maximum penetrations during the scratching), and 139.64 and 55.817 nm (the residual penetration depths calculated from AFM), respectively. It is revealed that only 20.61% and 39.97% of maximum penetration depths of A1 and A5 samples were remained. As a consequence of adding nano-HA particles into neat UHMWPE, the hardness of the materials in the direction of scratches were also improved, while the maximum penetration depths were decreased.

CONCLUSIONS

The nanoindentation and nanoscratching tests were used to investigate the nanomechanical and tribological properties of HA/UHMWPE nanocomposites. From the above discussion, the following important conclusions can be drawn:

1. The idea behind choosing nano-HA was that the addition of this bioceramic will improve the nanomechanical and tribological properties of UHMWPE polymer as a bone substitute biomaterial. Also, adding this bioceramic will provide bioactive sites on the surface of UHMWPE polymer, which can be filled with osteoblast cells and hence could be bioresorbed and replaced by natural bone cells.
2. Incorporation of nano-HA into pure UHMWPE results in remarkable enhancements in the elastic modulus and hardness of the nanocomposites.
3. The elastic modulus of A5 nanocomposite is less than cortical human bone and more than spongy human bone. Therefore, it is not suitable for spongy bone substitute, due to the stress shielding effect. On the other site, the A1 composite has an elastic modulus (1.4 GPa) close to spongy bone (0.01–1.57 GPa); hence, in elastic modulus term, it seems it can be an appropriate candidate for spongy bone replacement.
4. Nano-HA particles reduced the friction coefficients of neat UHMWPE considerably (for example, a 38.86% decrease in friction coefficient by adding 50 wt % HA).

ACKNOWLEDGMENTS

REFERENCES

1. Shokrieh, M.; Hosseinkhani, M.; Naimi-Jamal, M. R.; Tourani, H. *Polymer Testing* **2013**, *32*, 45.
2. Ferencz, R.; Sanchez, J.; Blümich, B.; Herrmann, W. *Polymer Testing* **2012** *31*, 425.
3. Liao, Q.; Huang, J.; Zhu, T.; Xiong, C.; Fang, J. *Mech. Mater.* *2012* **2010**, *42*, 1043.
4. Jee, A.-Y.; Lee, M. *Polymer Testing* **2010**, *29*, 95.
5. Sattari, M.; Naimi-Jamal, M. R.; Khavandi, A. *Polymer Testing* **2014**, *38*, 26.
6. Oliver, W. C.; Pharr, G. M. *J. Mater. Res. Pittsburgh Warrendale* **2004**, *19*, 3.
7. Tranchida, D.; Piccarolo, S.; Loos, J.; Alexeev, A. *Appl. Phys. Lett.* **2006**, *89*, 171905.
8. Kaupp, G.; Naimi-Jamal, M. R. *Scanning* **2013**, *35*, 88.
9. Kaupp, G. Atomic force microscopy, scanning nearfield optical microscopy and nanoscratching: application to rough and natural surfaces; Springer Science & Business Media: Springer-Berlin Heidelberg, Germany, **2006**.
10. Wang, M.; Hench, L.; Bonfield, W. *J. Biomed. Mater. Res.* **1998**, *42*, 577.
11. Wang, M.; Porter, D. *Br. Ceramic Trans.* **1994**, *93*, 91.
12. Knowles, J.; Bonfield, W. *J. Biomed. Mater. Res.* **1993**, *27*, 1591.
13. Bonfield, W. *Ann. N Y Acad. Sci.* **1988**, *523*, 173.
14. Zhou, J.; Yan, F. *J. Appl. Polymer Sci.* **2005**, *96*, 2336.
15. Li, W.; Guan, C.; Xu, J.; Mu, J.; Gong, D.; Chen, Z.-r.; Zhou, Q. *Polymer* **2014**, *55*, 1792.
16. Panin, S.; Kornienko, L.; Sonjaitham, N.; Tchaikina, M.; Sergeev, V.; Ivanova, L.; Shilko, S. *J. Nanotechnol.* **2012**, *7*, 2012.
17. Pinchuk, L. Proceedings of the 14th International Colloquium Tribology, Technische Academie Esslingen, Ostfildern, **2004**, pp 5.
18. Pinchuk, L.; Chernyakova, Y. M.; Goldade, V. *J. Friction Wear* **2008**, *29*, 224.
19. Tretinnikov, O. N.; Ikada, Y. *J. Polymer Sci. Part B: Polymer Phys.* **1998**, *36*, 715.
20. Mano, J. F.; Sousa, R. A.; Boesel, L. F.; Neves, N. M.; Reis, R. L. *Composites Sci. Technol.* **2004**, *64*, 789.
21. Hazar yoruÇ, A.; Karakaş, A.; Koyun, A.; Yildiz, T. *Acta Phys. Polonica A* **2012**, *121*, 3.
22. Santos, J. C.; Vieira, L. M.; Panzera, T. H.; Schiavon, M. A.; Christoforo, A. L.; Scarpa, F. *Mater. Des.* **2014**, *65*, 7.
23. Bonfield, W.; Grynpas, M.; Tully, A.; Bowman, J.; Abram, J. *Biomaterials* **1981**, *2*, 185.
24. Homaeigohar, S. S.; Sadi, A. Y.; Javadpour, J.; Khavandi, A. *J. Eur. Ceramic Soc.* **2006**, *26*, 273.
25. Ramakrishna, S.; Mayer, J.; Wintermantel, E.; Leong, K. W. *Composites Sci. Technol.* **2001**, *61*, 1189.
26. Fang, L. Hong Kong University of Science and Technology; **2003**.

27. Knets, I.; Bunina, L.; Filipenkov, V. *Mech. Composite Mater.* **1993**, *29*, 181.

28. Filipenkovs, V.; Laizans, J.; Knets, I. *Acta Bioeng. Biomech.* **2006**, *8*, 19.

29. Gul, R. M.; Mcgarry, F. *J Polymer Eng. Sci.* **2004**, *44*, 1848.

30. Oliver, W. C.; Pharr, G. M. *J. Mater. Res.* **1992**, *7*, 1564.

31. Li, X.; Bhushan, B. *Scr. Mater.* **2002**, *47*, 473.

32. Poveda, R.; Gupta, N.; Porfiri, M. *Mater. Lett.* **2010**, *64*, 2360.

33. Briscoe, B.; Fiori, L.; Pelillo, E. *J. Phys. D: Appl. Phys.* **1998**, *31*, 2395.

34. Sattari, M.; Molazemhosseini, A.; Naimi-Jamal, M. R.; Khavandi, A. *Mater. Chem. Phys.* **2014**, *147*, 942.

35. Tourani, H.; Molazemhosseini, A.; Khavandi, A.; Mirdamadi, S.; Shokrgozar, M. A.; Mehrjoo, M. *Polymer Composites* **2013**, *34*, 1961.

36. Abadi, M.; Ghasemi, I.; Khavandi, A.; Shokrgozar, M.; Farokhi, M.; Homaeigohar, S. S.; Eslamifar, A. *Polymer Composites* **2010**, *31*, 1745.

37. Suwanprateeb, J.; Tanner, K.; Turner, S.; Bonfield, W. *J. Biomed. Mater.* **1998**, *39*, 16.

38. Suwanprateeb, J.; Tanner, K.; Turner, S.; Bonfield, W. *J. Mater. Sci.: Mater. Med.* **1997**, *8*, 469.

39. Weiner, S.; Wagner, H. D. *Ann. Rev. Mater. Sci.* **1998**, *28*, 271.

40. Rho, J.-Y.; Kuhn-Spearing, L.; Zioupos, P. *Med. Eng. Phys.* **1998**, *20*, 92.

41. Zysset, P. K.; Edward Guo, X.; Edward Hoffler, C.; Moore, K. E.; Goldstein, S. A. *J. Biomech.* **1999**, *32*, 1005.

42. Norman, J.; Shapter, J. G.; Short, K.; Smith, L. J.; Fazzalari, N. L. *J. Biomed. Mater. Res. Part A* **2008**, *87*, 196.

43. Rho, J. Y.; Roy, M. E.; Tsui, T. Y.; Pharr, G. M. *J. Biomed. Mater. Res.* **1999**, *45*, 48.

44. Zysset, P. K.; Edward Guo, X.; Edward Hoffler, C.; Moore, K. E.; Goldstein, S. A. *J. Biomechan.* **1999**, *32*, 1005.

45. Molazemhosseini, A.; Tourani, H.; Naimi-Jamal, M. R.; Khavandi, A. *Polymer Testing* **2013** *32*, 525.

46. Fischer-Cripps, A. C. Nanoindentation; Springer Science & Business Media: New York, **2011**.

47. Kogut, L.; Etsion, I. *J. Tribol.* **2004**, *126*, 34.

48. Nakajima, A.; Mawatari, T. *Tribol. Ser.* **1998**, *34*, 291.

49. Mai, K.; Mäder, E.; Mühle, M. *Composites Part A: Appl. Sci. Manufact.* **1998**, *29*, 1111.

50. Adam, C. J.; Swain, M. V. *J. Mech. Behav. Biomed. Mater.* **2011**, *4*, 1554.

51. Shockey, J. S.; von Fraunhofer, J. A.; Seligson, D. *Surface Technol.* **1985**, *25*, 167.